JACS
JOURNAL OF THE AMERICAN CHEMICAL SOCIETY

ARTICLE

pubs.acs.org/JACS

Chemical Shifts for the Unusual DNA Structure in Pf1 Bacteriophage from Dynamic-Nuclear-Polarization-Enhanced Solid-State NMR Spectroscopy

Ivan V. Sergeyev,[†] Loren A. Day,[‡] Amir Goldbourt,[§] and Ann E. McDermott*[,†]

[†]Department of Chemistry, Columbia University, 3000 Broadway, New York, New York 10027, United States

[‡]The Public Health Research Institute of the University of Medicine and Dentistry of New Jersey, 225 Warren Street, Newark, New Jersey 07103, United States

[§]School of Chemistry, Raymond and Beverly Sackler Faculty of Exact Sciences, Tel Aviv University, Ramat Aviv 69978, Tel Aviv, Israel

Supporting Information

ABSTRACT: Solid-state NMR spectra, including dynamic nuclear polarization enhanced 400 MHz spectra acquired at 100 K, as well as non-DNP spectra at a variety of field strengths and at temperatures in the range 213−243 K, have allowed the assignment of the ^{13}C and ^{15}N resonances of the unusual DNA structure in the Pf1 virion. The ^{13}C chemical shifts of C3′ and C5′, considered to be key reporters of deoxyribose conformation, fall near or beyond the edges of their respective ranges in available databases. The ^{13}C and ^{15}N chemical shifts of the DNA bases have above-average values for AC4, AC5, CC5, TC2, and TC5, and below average values for AC8, GC8, and GN2, pointing to an absence of Watson−Crick hydrogen bonding, yet the presence of some type of aromatic ring interaction. Crosspeaks between Tyr40 of the coat protein and several DNA atoms suggest that Tyr40 is involved in this ring interaction. In addition, these crosspeak resonances and several deoxyribose resonances are multiply split, presumably through the effects of ordered but differing interactions between capsid protein subunits and each type of nucleotide in each of the two DNA strands. Overall, these observations characterize and support the DNA model proposed by Liu and Day and refined by Tsuboi et al., which calls for the most highly stretched and twisted naturally occurring DNA yet encountered.

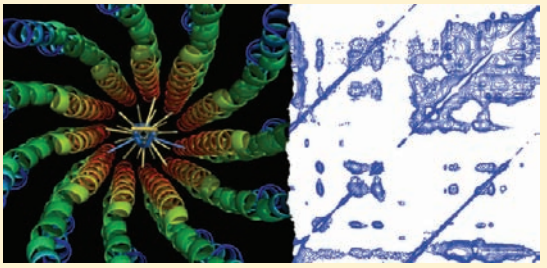

INTRODUCTION

Pf1, a 36 MDa filamentous circular single-stranded DNA bacteriophage specific to strain K of *Pseudomonas aeruginosa* (PAK),[1] is one of the innumerable filamentous phages comprising the genus *Inovirus*, many of which are integrative and some of which carry virulence factors that convert their bacterial hosts from nonpathogens into pathogens.[2−6] Although Pf1 itself is nonintegrative and carries no virulence factors, phages with Pf1-like structural genes are present as integrated prophages in other *Ps. aeruginosa* strains, some found in clinical isolates from cystic fibrosis patients.[7−9] Pf1 and Pf1-like virions are 7 nm in diameter, like virions of all inoviruses, but they are much longer than others of similar genome size due to the unusual, stretched conformation of the packaged circular single-stranded DNA. For example, the Pf1 genome of 7.3 kb[10] is packed in a virion about 2 μm long, whereas the well-known phages of the Ff group (f1, fd, M13) have 6.4 kb genomes packed in 0.9 μm long virions.[11,12] The circular genomes in such virions have two non-complementary DNA strands running in opposite directions from end to end, with the nature of strand−strand and strand−capsid interactions varying markedly among the different species. Thus, the structures of Pf1 and of other filamentous phages are of biomedical and fundamental biophysical interest.

Pf1 structure has become one of the paradigms for filamentous phages in that its capsid symmetry of approximately 27 protein subunits in five helical turns is common to many inoviruses, as is the small size and high α-helicity of these subunits.[13] However, Pf1 has an unusual 1:1 ratio of nucleotides to major capsid subunits, rather than a ratio between 2.0 and 2.5 as in most other inoviruses. Of its 7349 nucleotides, ∼7300 interact with an equal number of gene 8 product (major coat protein) subunits.[11,14−17] On the basis of this 1:1 stoichiometry, and an electron density map of a low temperature form of Pf1,[18] as well as extensive spectroscopic data, a model has been developed in which the helical symmetries of DNA and capsid were matched (PDB: 1PFI).[12,19−21] The positions of OPO groups of the DNA (phosphorus plus nondiester oxygens) for the model as deduced by Liu and Day[12] from the electron density map[18] corresponded perfectly with prior electrostatic calculations,[20] and placed antiparallel sugar−phosphate chains at the center, with the phosphorus atoms at 2.5 Å radius and phosphorus−phosphorus distances of 7.5 Å within strands and 5.2 Å between strands. Also, the model has the nondiester OPO planes uniformly

Received: May 10, 2011
Published: August 22, 2011

ACS Publications © 2011 American Chemical Society

oriented, the deoxyribose puckers uniformly C2′-endo/*gg*, the base-sugar orientations *anti*, and the base planes approximately parallel to the axis. Subsequently, M. Tsuboi and co-workers[21−23] confirmed these features and contributed significant additions and refinements, especially with respect to the average orientations of all four individual bases. DNA structures closely resembling that of highly stretched and twisted Pf1 DNA have been generated by single-molecule techniques applied to double- and single-stranded DNA in solution.[24,25] Nevertheless, the complete structure of the Pf1 virion has been controversial, and is still puzzling with respect to its dynamics[26] and an inherent polymorphism stemming from the fact that its capsid subunits are all oriented in one direction while the two DNA strands run in opposite directions. The unresolved problems require an atomic level high-resolution study.

Magic angle spinning solid-state NMR (MAS-SSNMR) is a powerful tool for the study of biopolymers, even in cases where they are in very large assemblies, nanocrystalline, frozen, or aggregated.[27,28] Nearly complete atomic level assignments of protein resonances have been accomplished for over a dozen systems in the solid state using multidimensional heteronuclear (^{13}C, ^{15}N) MAS-SSNMR, and can provide valuable insight into the structure and dynamics of a molecule.[28−30] A number of proteins have been assigned in this manner, including ubiquitin,[31,32] GB1,[33] SH3,[34] LH2,[35] kaliotoxin,[36] Crh,[37] thioredoxin,[38] BPTI,[39] and others. Such assignments have led to three complete tertiary structures, and a number of partial structures.[36,40−43] Nucleic acids have also been studied by SSNMR, albeit to a lesser degree. A number of small nucleic acid constructs have been studied by SSNMR,[44−48] with a notable recent high-resolution study of a ^{13}C,^{15}N-labeled RNA tetraloop in frozen solution,[49] but no detailed structural work has been published on longer nucleic acid sequences. Significant difficulty in probing nucleic acid structure by SSNMR stems from two basic problems: most nucleotides have very similar chemical shifts, leading to spectral congestion, and it is rather difficult to transfer magnetization between neighboring nucleotides due to their phosphate linkage and the distances involved. However, valuable structural information can still be extracted using chemical shift analysis.

Previous studies of Pf1 by SSNMR have focused primarily on the major coat protein, generally considered to have a single structure shared by all ∼7300 subunits. Opella et al. reported a distinct kink at residue 29 and an unusual "double hook" for the 6 N-terminal residues,[50] along with a few small changes in the backbone between low- and high-temperature forms of Pf1, despite significant changes in the spectra.[51] Goldbourt et al.[52] have reported an assignment of the coat protein that was close to complete, defining additional constraints for the subunit, including the presence of more than one resonance from a few atoms, and Lorieau et al. have reported on remarkable protein conformational dynamics.[26] Previous ^{31}P NMR[53−55] studies have examined the DNA of Pf1 and Ff (fd and M13) filamentous phages to reveal notable differences. To our knowledge there have been no studies of the ^{13}C and ^{15}N chemical shifts of the DNA sugars and bases. We present here the first high-resolution NMR study of the DNA of the Pf1 bacteriophage.

RESULTS

Dynamic nuclear polarization (DNP) SSNMR spectra, acquired with sample temperatures of approximately 100 K, have, for the first time, allowed us to resolve and assign the DNA of Pf1 in high-resolution spectra. These are compared to other high-resolution spectra of Pf1 acquired at a variety of field strengths without the benefit of DNP. Figure 1 shows the numbering scheme used for nucleotide bases as well as the current completeness of assignment. Assignments of the DNA were initially made based on available chemical shift data,[56,57] followed by "sequential walks" between assigned peaks via their mutual crosspeaks to map out the nucleotide spin systems. Figure 2a,b shows the assignments of the dC/dT and dA/dG spin systems, respectively, while Figure 2c shows the assignments of the sugar resonances. The full spectrum [dipolar assisted rotational resonance (DARR) with 22 ms mixing time] may be seen in Figure S1. Table 1 provides a table of the measured chemical shifts compared to biological magnetic resonance data bank (BMRB) averages. Current assignments are at the level of nucleotide type.

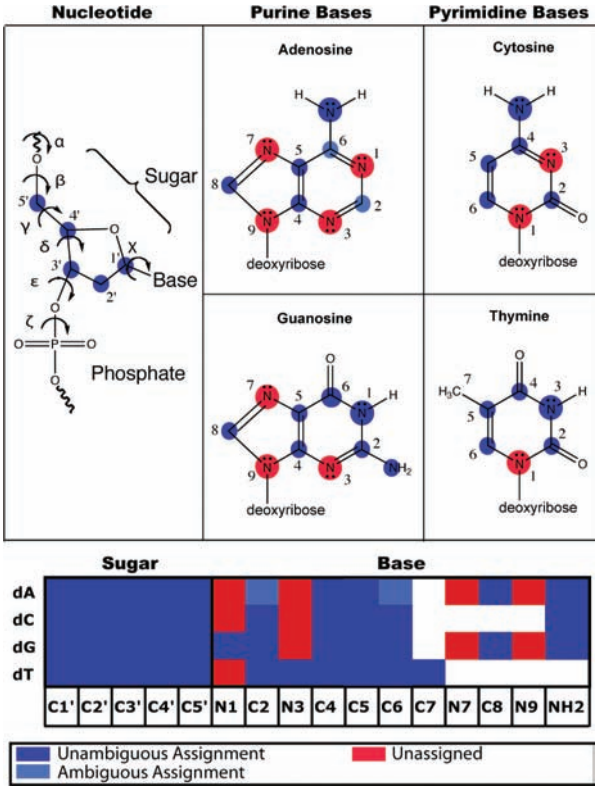

Figure 1. Numbering scheme for nucleotide sugars and bases to be used throughout this paper, as well as the common nomenclature of the sugar torsion angles. Colored circles in the top pane, in addition to the bottom graphic, illustrate the current extent of assignment for Pf1 DNA.

The current ^{13}C assignment of the DNA bases (19/19 assigned), and the DNA sugars (5/5 assigned) is complete; however, due to chemical shift range overlap and a lack of strong crosspeaks, two of the base resonance assignments (2/19, 10.5%) remain ambiguous. Current data do not allow us to differentiate sugar chemical shifts arising from the different nucleotides with the exception of TC1′, TC3′, and TC4′, which have been assigned on the basis of their crosspeaks with TC7. Due to the use of cross-polarization from protons, and the mechanism of polarization enhancement in DNP (the cross effect or three-spin thermal mixing, both of which typically involve protons[58]), it is not surprising that nuclei in proton-poor environments receive little magnetization and are difficult to observe.[55] Further, there is significant spectral overlap in the ^{13}C chemical shift region corresponding to the DNA bases, attributable both to strong

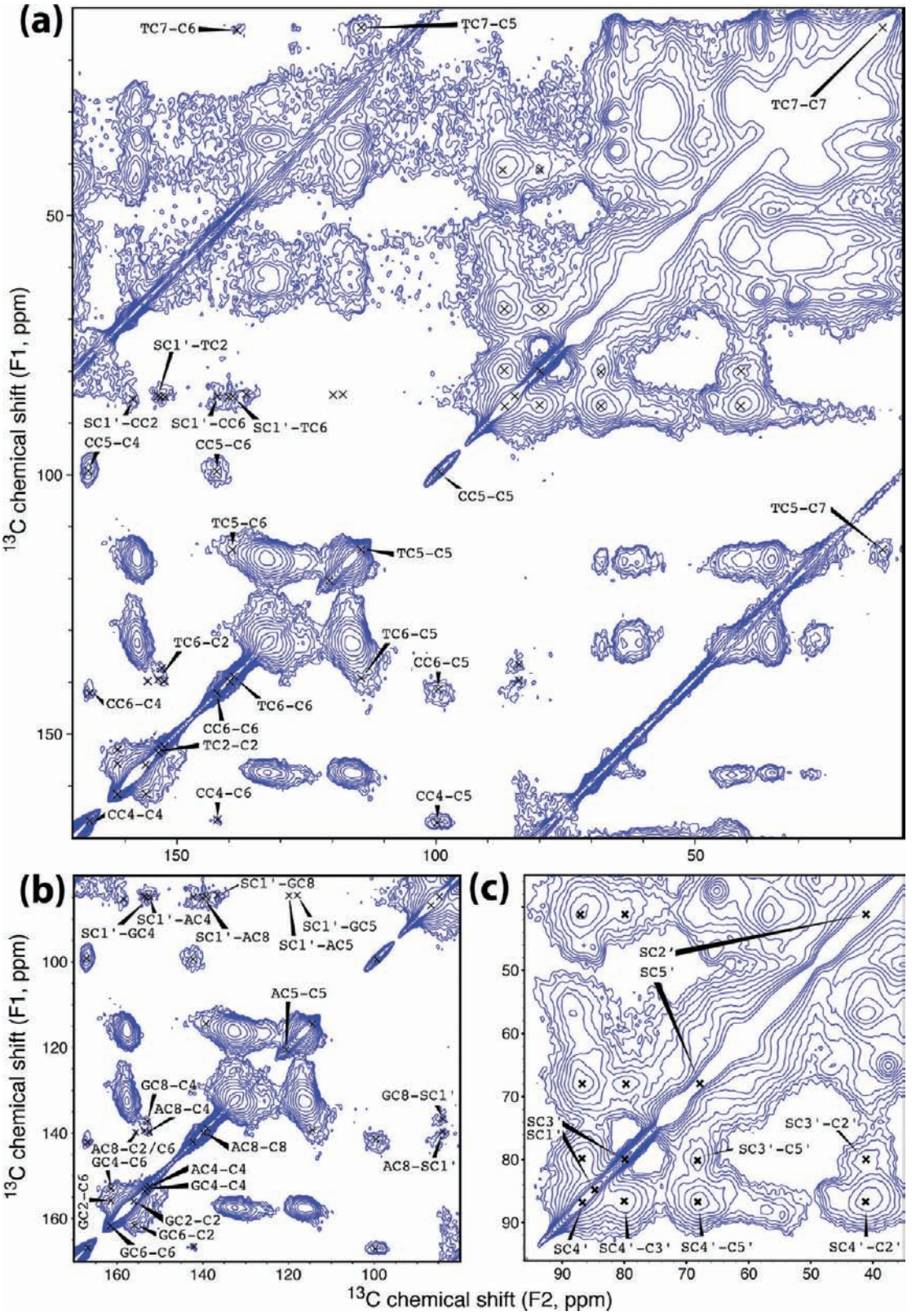

Figure 2. DNP-enhanced SSNMR spectra of Pf1 showing (a) the assignments of the dC/dT base resonances, (b) the dA/dG base resonances, and (c) the sugar spin systems. Data were collected using a 400 MHz wide-bore AVANCE III spectrometer at cryogenic temperatures (100 K), with a mixing time of 22 ms. See Table S1 for additional acquisition and processing parameters.

tyrosine peaks from the coat protein and to closely spaced chemical shifts. Resonances with low signal-to-noise may thus be obscured by more intense peaks and require additional enhancement to be resolvable. Some crosspeaks that were

Table 1. Comparison of Experimental Pf1 Chemical Shift Values to the Minimum, Maximum, and Average DNA Chemical Shift Values Obtained from Three Data Sources: The BMRB (Diamagnetic Only), Averages for Small Molecules, and Averages for B-Form Oligomers

	BMRB DNA[a]				B-DNA (C2′-endo)[b]				small mol.[c]		experimental				
	min	max	av	std dev	min	max	av	std dev	min	max	DNP 400 MHz, −173 °C	750 MHz, −30 °C	900 MHz, −60 °C	400 MHz, −35 °C	DNA-labeled 750 MHz, −30 °C
SC1′	82.9	88.5	86.5	1.5	81.7	88.4	84.3	1.6	83	89	84.8	86.0	84.8	85.9	85.6−89.9
SC2′	36.2	44.4	41.1	1.4	36.0	42.7	40.2	1.2	35	38	41.1	41.0	40.4	40.4	38.6−42.3
SC3′	71.9	81.7	77.9	2.1	69.7	80.7	76.9	2.2	70	78	79.9	79.9	79.9	80.0	77.0−81.7
SC4′	83.9	89.4	86.7	2.3	83.1	89.8	86.3	1.6	82	86	86.8	87.2	86.5	87.0	85.6−89.9
SC5′	63.3	69.7	66.9	3.2	64.0	68.6	67.2	1.3	63	68	67.9	68.7	67.6	68.7	67.0−69.1
AC2	153.1	155.7	155.1	0.7	150.5	155.4	153.7	1.3	152	156	156.5[d]			156.5[d]	
AC4					146.9	151.1	149.7	2.4	149	151	152.4			153.1	
AC5					116.4	120.8	118.6	3.1	119	121	120.3		121.1	121.5	
AC6					154.1	158.0	156.7	2.2	157	158	156.5[d]			156.5[d]	
AN6	77.4	81.7	80.2	1.4					82	84	82.4				
AC8	139.0	142.7	141.7	0.6	138.3	142.5	140.7	1.3	137	142	140.0	139.7	140.3	140.5	
CC2					159.3	159.8	159.5	0.4	159	159	158.5	159.5	159.7	159.1	
CC4					168.3	168.6	168.5	0.2	166	168	167.2	167.9	166.9	168.2	
CN4	95.1	98.6	97.4	1.1					94	98	97.5				
CC5	97.4	99.2	98.7	0.4	96.7	99.6	98.4	0.8	94	99	99.4	98.7	98.8	98.8	
CC6	141.6	144.7	143.4	0.6	141.7	144.0	142.9	0.8	136	144	142.0	141.4	142.0	141.3	
GN1	146.7	147.7	147.0	0.3					146	149	148.1				
GC2					156.3	156.5	156.4	0.2	156	156	155.9	155.8	155.9		
GN2	75.1	75.6	75.4	0.2					72	76	74.4				
GC4					153.5	153.7	153.6	0.1	152	154	153.0	153.1		153.0	
GC5					118.3	119.0	118.6	0.5	117	119	117.9			119.0	
GC6					161.0	161.4	161.2	0.2	161	161	161.6	161.4			
GC8	136.1	139.9	138.9	0.9	135.8	139.8	138.0	1.2	131	138	136.6		136.1	135.9	
TC1′	84.8	87.9	87.2	0.7	83.1	86.3	84.5	1.1	83	89				86.0	
TC3′	73.4	79.9	77.5	1.5	73.5	79.4	76.7	1.8	70	78				80.7	
TC4′	84.6	88.5	86.2	0.9	83.2	86.7	85.0	1.5	82	86				87.2	
TC2					148.5	153.2	151.6	2.7	154	154	153.5		153.2	153.8	
TN3	158.4	160.5	159.3	0.8					156	156	158.7				
TC4					164.9	168.1	166.8	1.6	169	169		167.5		166.4	
TC5	*e*	*e*	*e*	*e*	109.2	113.6	112.1	2.5	95	112	114.4	114.4	113.1		
TC6	137.2	140.1	139.4	0.5	134.9	139.8	138.2	1.4	137	142	138.9	138.5	138.5	140.2	
TC7	13.5	14.8	14.3	0.4	10.4	14.6	13.7	1.3	15	20	13.7	14.2	14.1	15.2	

[a] Ref 56. [b] See Supporting Information for data sources. [c] Ref 57. [d] Ambiguous assignment. [e] TC7 is occasionally termed the C5-methyl, leading to erroneous chemical shift entries in the BMRB for both TC5 and TC7.

notably absent in the 22 ms DARR spectrum were subsequently found in the 100 ms DARR spectrum, allowing us to confirm their initially ambiguous assignments via sequential walk. As an additional note, 5 of the expected 19 DNA ^{15}N resonances are currently assigned.

SSNMR data acquired at 213−243 K without DNP (at ^{1}H fields of 400, 750, and 900 MHz, shown in Figure 3 and in Figures S2−S4) also showed many of the DNA diagonal and cross-peak resonances observed in the DNP spectra, albeit at significantly lower intensity. The increased resolution of these data sets allowed us to assign unambiguously GC2 and GC4, which were hidden in a congested region of the DNP spectrum, and provided confirmation that the chemical shifts at the cryogenic temperatures used for DNP agree with those measured at temperatures closer to those of previous structural studies of Pf1^{L} within an average of 0.3 ppm, with a maximum of 1.3 ppm. A direct comparison of linewidths with DNP spectra is not appropriate in this case due to both differing field strengths and temperatures.

A sparsely labeled sample was also prepared by providing natural abundance amino acids to *P. aeruginosa* during the inoculation stage (see Materials and Methods) so as to suppress isotopic labeling of the coat protein as much as possible, while retaining isotopic labeling of the DNA by including U−^{13}C glucose. Under these conditions the DNA bases appear to be largely natural abundance (mainly ^{12}C), and the signals that were observed were primarily due to DNA deoxyriboses, which allowed us to confirm their assignments. Analysis of the observed splitting patterns also provided additional evidence of local microheterogeneity in the DNA sugars. The ^{13}C−^{13}C DARR spectrum of this sparsely labeled sample is available in Figure S5.

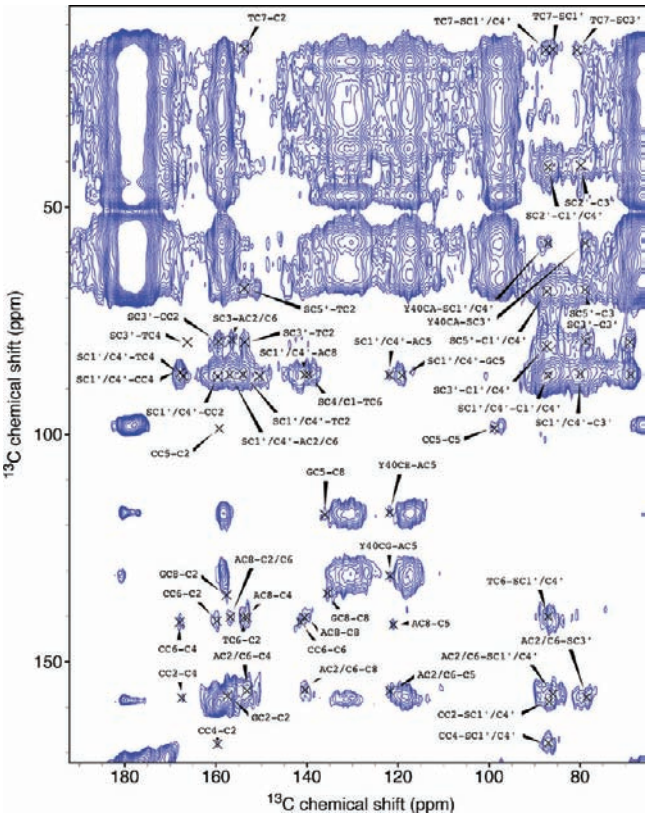

Figure 3. 2D DARR (200 ms mixing time) spectrum of U−^{13}C,^{15}N Pf1, acquired at 400 MHz and −35 °C.

DISCUSSION

Chemical Shift Analysis. The NMR data on DNA in Pf1 exhibit unusual chemical shift patterns. Ribose chemical shifts have been reported to be excellent reporters of conformation, those of C3′ shifting as much as 10 ppm between C2′-endo and C3′-endo conformers.[56] Lankhorst and co-workers found that a transition from S-type (C2′-endo, C3′-exo) to N-type (C3′-endo, C2′-exo) pucker would result in downfield shifts of C1′ and C2′, while C3′ and C4′ would shift upfield.[59] Santos and co-workers found large (averages of 7.4 and 4.7 ppm, respectively) upfield shifts at both the C3′ and C5′ positions in going from C2′-endo to C3′-endo sugar pucker.[60] Au-Yeung et al.[61] subsequently identified three distinct regions of conformational space, primarily dictated by the sugar pucker backbone torsion angle γ, with 3′-endo/*gauche* conformations having C3′ chemical shifts <70 ppm, 3′-endo/*trans* and 2′-endo/*trans* conformers falling between 70 and 74 ppm, and 2′-endo/*gauche* conformers >74 ppm. Further, a change in the backbone torsion angle γ from *gauche* to *trans* results in a downfield shift of the C5′ resonance by 4−5 ppm. C2′ and C4′ chemical shifts are useful in distinguishing between the relatively similar C2′-endo and C3′-exo conformations, with higher chemical shifts observed in the C2′-endo case at both positions.[60] The sugar chemical shifts can also serve as reporters of the glycosidic angle (χ), with Greene and co-workers reporting modest downfield shifts for C1′, C3′, and C4′ and dramatic upfield shifts at the C2′ position in going from *anti* to *syn* orientations.[62]

Chemical shifts of the DNA bases, though not known to be strong reporters of conformation, can still provide some valuable insight. Ghose and co-workers predict C8 chemical shifts to be good reporters of conformation for the glycosidic torsion, with *syn* conformations being shifted significantly downfield of *anti* conformations.[63] This was corroborated by the experimental shifts of Greene and co-workers, who also observed a modest downfield shift of C4 and C5, with a larger effect on C5 (averaging 0.65 and 1.15 ppm, respectively) for all bases in *syn* conformations.[62] Lam and Chi note that guanosine C4 and C5 chemical shifts are especially prone to downfield shifts in *syn* conformations.[64] Perhaps more importantly, ^{13}C chemical shifts are sensitive both to base-pairing (H-bonding) and base-stacking. Borer et al., using a series of oligonucleotide duplexes, showed that six ^{13}C nuclei, those of GC2, GC6, TC4, TC7, CC5, and AC6, drift toward higher chemical shifts in response to Watson−Crick base-pair formation, presumably due to additional shielding from increased ring currents and steric compression effects, while the remaining DNA base resonances, especially those of GC5, GC8, CC6, AC2, AC5, and TC2, are shifted upfield.[65] The predicted downfield shifts of GC2, GC6, and TC4 upon H-bond formation are borne out by the melting data of LaPlante et al.[66] Farès et al. observed a slightly different pattern in RNA, noting that AC2, AC4, AC8, GC4, GC8, CC5, CC6, UC2, UC5, and UC6 are all shifted downfield by disruption of base-pairing and base-stacking, while only UC4 is shifted upfield. Many of these findings are corroborated by contrasting the BMRB chemical shift trends of nucleotides in disordered and ordered regions. Further, it has been found that the disruption of base-pairing and base-stacking often have cooperative effects upon chemical shift.[67] Finally, Malináková et al., in a recent detailed density functional theory (DFT) study of the chemical shift tensors of purine bases, find that the C4, C5, and C6 carbons are somewhat insensitive to the effects of base-pairing while C2 and C8 shift downfield dramatically with the addition of hydrogen bonds. C5 and C6 are however quite sensitive to base-stacking, shifting downfield by as much as 3 ppm when stacked bases are present, while C2, C4, and C8 are insensitive to this effect.[68]

On the basis of the experimental chemical shifts, we conclude that Pf1 DNA exhibits a 2′-endo/*gauche* conformation because of its high C3′ chemical shift (79.9 ppm) and its above-average C5′ chemical shift (67.9 ppm). We have compared these values to B-DNA averages (76.9 ± 2.2 ppm for C3′ and 67.2 ± 1.3 ppm for C5′, see Supporting Information for data sources) and the averages for all DNA from the BMRB (77.9 for C3′ and 66.9 for C5′). The average Pf1 DNA chemical shifts for C2′ (41.1 ppm) and for C4′ (86.8 ppm) also point to a C2′-endo conformation, and are not consistent with C3′-exo. In addition, below-average A/GC8 and GC4 shifts along with a low GC5 shift all suggest an *anti* conformation for the glycosidic torsion, consistent with previous reports.[21,23]

As can be seen in Table 1, several of the resonances assigned to the DNA bases of Pf1 lie outside of the "normal" ranges found in the BMRB, and more than one standard deviation from their respective mean in a database derived from B-form oligonucleotide data, consistent with an unusual structure. Both BMRB data and oligonucleotide data are either unavailable or very sparse for some of the DNA base resonances due to a lack of data: in these cases, chemical shift ranges derived from small molecule studies are provided for comparative purposes. It should be noted however that small molecule experiments likely lack many of the interactions present in lengthier nucleic acids and so may yield a less reliable set of chemical shifts. Currently available BMRB DNA ^{13}C chemical shift data represent an ensemble of

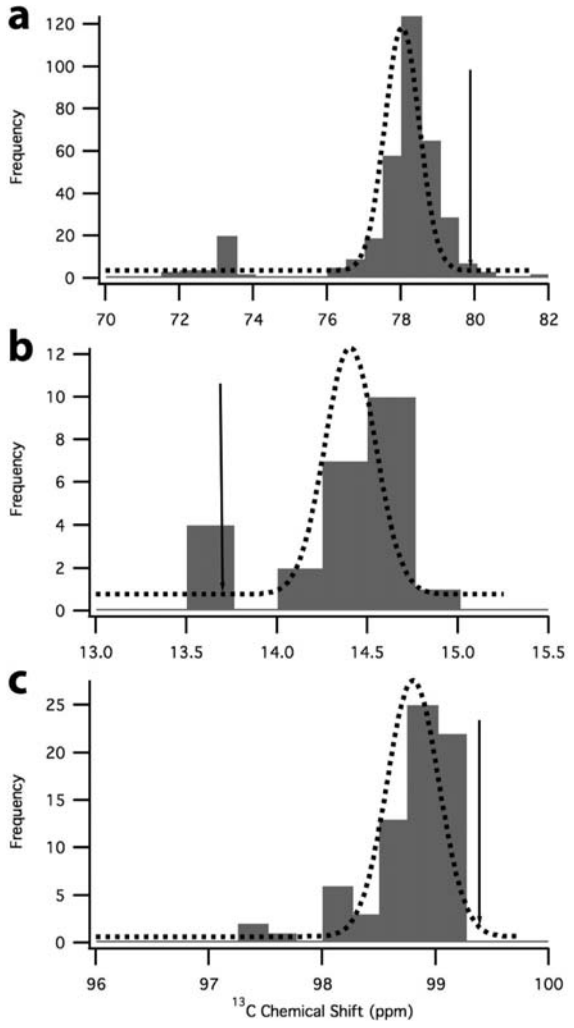

Figure 4. Histograms of all DNA ^{13}C chemical shifts for (a) C3′, (b) TC7, and (c) CC5 available in the BMRB are shown in gray. Gaussian curve fits of the histograms are shown as dashed lines, and are provided solely to illustrate approximate means and standard deviations. It should be noted that the populations are not normally distributed. The unusual chemical shifts observed in Pf1 DNA are denoted by solid vertical arrows at 79.9, 13.7, and 99.4 ppm, respectively.

27 structures. Of these, approximately half are random coil, with the rest being primarily B-type oligomers in DNA−protein complexes, along with a DNA hairpin, a quadruplex, and a tetraloop. As a result, the BMRB chemical shift averages and ranges should represent a fairly well-distributed sampling of possible conformations, though A- and Z-form DNA are conspicuously underrepresented. Of those atoms for which BMRB data are available, the DNP chemical shift for CC5 is 0.2 ppm above the upper end of its chemical shift range, and that of TC7 is almost two standard deviations below average, as can be seen in Figure 4. Strangely, the chemical shift of TC7 in one of the five data sets presented herein is 15.2 ppm, falling 0.4 ppm above the upper bound of its normal range; we are unable to explain this discrepancy. As for the rest, AC4, AC5, TC2 and TC5 all have unusually high chemical shifts significantly above their normal ranges. CC4, GC4, and GC5 have unusually low chemical shifts.

Unusually high chemical shift values for AC2, AC5, and TC2, together with below-average shifts for GC2 and TC7 (despite the outlier of 15.2 ppm as previously noted), are consistent with the absence of hydrogen bonding as seen in the experimental data of Borer et al. and LaPlante et al.[65,66] Further, the high chemical shifts of AC4, CC5, TC2, and TC5 are all consistent with the findings of Farès et al. for the disruption of base-pairing/base-stacking interactions.[67] Finally, when overlaid with the purine DFT results of Malináková et al., our observed above average AC5 chemical shifts are consistent with some sort of base-stacking, while below average A/GC8 chemical shifts are indicative of decreased or disrupted base-pairing.[68] These findings are also reinforced by ^{15}N chemical shifts; Jones et al. report a 4 ppm upfield shift for guanine amino groups (GN2) upon melting.[69] While not as dramatic as 4 ppm, GN2 in Pf1 is 0.7 ppm below the BMRB minimum. Taken together, these analyses of the DNA base chemical shifts of Pf1 are consistent with a highly unusual structure, namely one with little or no base-pairing, as concluded by previous studies,[11,14,70] but with some sort of base-stacking. If it is considered that the effects of DNA base-stacking on chemical shifts could be closely mimicked by $\pi-\pi$ interactions between a DNA base and an adjacent tyrosine (as is consistent with UV and CD spectra, as well as observed Tyr40 fluorescence quenching and an undefined pK_a for Tyr40), this is exactly as would be expected from the model put forth by Liu and Day.[12] Further, cation$-\pi$ interactions are expected between the DNA bases and residues R44 and K45 of the coat protein, though their effects on the ^{13}C chemical shifts of the DNA are difficult to predict.[71]

DNP Enhancement and Pulse Sequence. DNA peaks observed in DNP spectra have approximately one-fifth the signal intensity of coat protein peaks, and hence suffer from a lack of signal-to-noise in non-DNP enhanced SSNMR experiments. While these peaks had been faintly observable previously, their assignment had been nearly impossible due to poor line shape, spectral overlap, and spectral noise. Even with extremely dense (>500 mg/mL) preparations, the sensitivity of detection of these peaks remains borderline. With enhancement, however, these peaks are clearly distinguishable and assignable. DNP provides an order of magnitude increase in sensitivity, increasing signal-to-noise ratio approximately 16.6-fold and intensity approximately 21.6-fold. Figure S6 shows the enhancement ratio as calculated using different regions of the spectrum. DNP has been previously shown to be successful for bacteriophages,[72] and standard protocols were followed in sample preparation and data acquisition. Additional enhancement may yet be possible using other solvent/biradical combinations. The linewidths of the DNP-enhanced spectra (minimum 1.8 ppm/179 Hz, average 2.4 ppm/238 Hz) are however considerably broader than those of spectra taken at −35 °C and comparable field strength (average 1.4 ppm/138 Hz), presumably due to additional sample heterogeneity stemming from the cryogenic temperatures.

It has also been noted that the intensities of some DNA ^{13}C homonuclear crosspeaks can be heavily dependent on the choice of pulse sequence. This can be attributed to proton-poor chemical environments, which may preclude efficient magnetization transfer to certain nuclei in generic cross-polarization (CP) based pulse sequences such as DARR.[73] Spectra were acquired using the standard DARR (with CP element) pulse sequence as well as a variant where the ^{1}H 90 deg. pulse and CP elements were replaced with a simple ^{13}C 90 deg. pulse (1pulse-DARR). Comparative spectra taken with the former and latter pulse sequences can be seen in Figure S7. The peak corresponding to TC5, for instance, is notably enhanced in the 1pulse-DARR

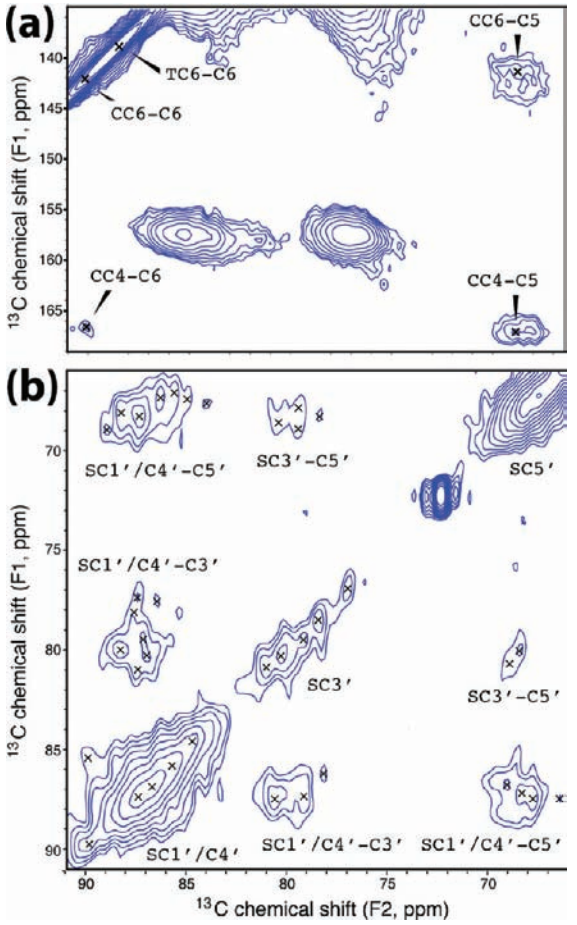

Figure 5. Peak splitting in Pf1 2D $^{13}C-^{13}C$ spectra as illustrated by (a) the CC4-CC5 crosspeak in the DNP-DARR (100 K, 22 ms mixing time) spectrum of U$-^{13}C,^{15}N$ Pf1 and (b) the sugar peaks in the DARR spectrum (240 K, 50 ms mixing time) of DNA-$^{13}C,^{15}N$ Pf1. The splittings indicate at least 5 distinct chemical shifts for each of C1′/C4′, C3′, and C5′.

spectrum, presumably because it is proton-poor and therefore does not receive sufficient magnetization via CP and mixing.

Peak Splitting. Linewidths and substructure in individual crosspeaks can sometimes be a useful reporter of structural heterogeneity, particularly at low temperatures when conformational heterogeneity may be present (an ensemble of different static conformers).[74] Our DNP data were collected on a 400 MHz Bruker spectrometer at cryogenic temperatures of approximately 100 K. Different linewidths were observed. While certain peaks had linewidths below 2 ppm (i.e., Ile26 Cα-Cδ, full width at half-height (fwhh) = 1.8 ppm), most others were broader. Diagonal peaks had typical linewidths of 3 ppm, and off-diagonal peaks had average fwhh of 4.5 ppm, with a maximum of 6 ppm. These differences in the crosspeak linewidths would be consistent with static heterogeneity in the local environment, a finding that holds true for both the DNA and some coat protein sites. Despite the broad peaks, some peaks look distinctly doublet-like, such as the C4−C5 crosspeak of deoxycytidine in Figure 5a. Such splitting effects are very pronounced for the sugar carbons. In the spectra of DNA-$^{13}C,^{15}N$-labeled Pf1 taken at 750 MHz, all sugar resonances are split into several peaks (5 or more) as shown in Figure 5b. Splittings in the DNA sugar resonances may well also propagate to the phosphorus of the phosphate groups,

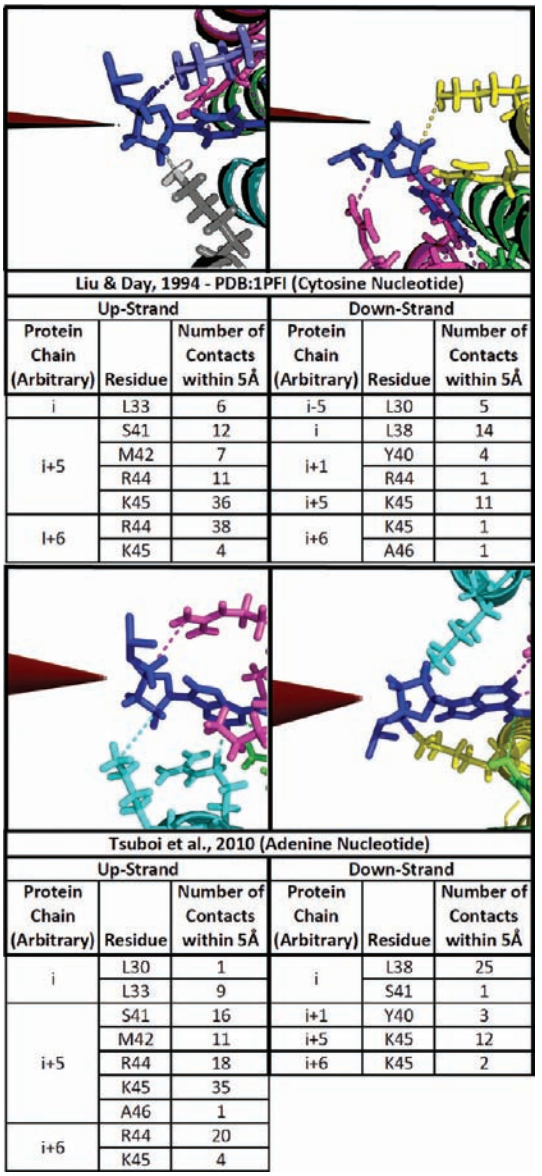

Liu & Day, 1994 - PDB:1PFI (Cytosine Nucleotide)

Up-Strand			Down-Strand		
Protein Chain (Arbitrary)	Residue	Number of Contacts within 5Å	Protein Chain (Arbitrary)	Residue	Number of Contacts within 5Å
i	L33	6	i-5	L30	5
i+5	S41	12	i	L38	14
	M42	7	i+1	Y40	4
	R44	11		R44	1
	K45	36	i+5	K45	11
i+6	R44	38	i+6	K45	1
	K45	4		A46	1

Tsuboi et al., 2010 (Adenine Nucleotide)

Up-Strand			Down-Strand		
Protein Chain (Arbitrary)	Residue	Number of Contacts within 5Å	Protein Chain (Arbitrary)	Residue	Number of Contacts within 5Å
i	L30	1	i	L38	25
	L33	9		S41	1
i+5	S41	16	i+1	Y40	3
	M42	11	i+5	K45	12
	R44	18	i+6	K45	2
	K45	35			
	A46	1			
i+6	R44	20			
	K45	4			

Figure 6. Graphic showing interactions between representative nucleotides in up- and down-strands of Pf1 DNA and their nearest coat protein subunits, based on coordinates from Liu and Day [PDB: 1PFI][12] (upper panel) and Tsuboi et al.[21] (lower panel). Each image is aligned looking up the central axis of the virion, shown as a projection of a red cylinder. Different colors are for different subunits, and closest contacts are denoted with dashed lines. The lists of contacts, restricted to heavy-atom contacts within 5 Å, demonstrate that up-strand and down-strand nucleotides have very different sets of first-shell neighbors, and that contacts are similar for the different nucleotide types. Note that the overlapping and interdigitation of subunits in the capsid lattice place the side-chains of at least three different protein subunits (i, i + 5, and i + 6) in contact with each nucleotide.

explaining the heterogeneity and broad ^{31}P resonances found in earlier studies.[53,75]

Several residues in the coat protein also exhibit multiple peaks, as observed in high-resolution $^{13}C-^{13}C$ homonuclear DARR spectra at 240 and 273 K. These include Y40 (more specifically its ring atoms), M42, and R44, all in the DNA-binding C-terminal domain of the subunit. T5 in the N-terminal region has also been observed to exhibit multiple resonances. For all other coat

protein residues, however, we observe one peak per atom at resolutions well below 1 ppm, indicating that all copies of the coat protein share the same overall conformation.[52,26] Surprisingly, order parameters observed for the side chains of residues R44 and K45 in the C-terminal DNA-binding region were low, on par with those of residues in the N-terminal region exposed to solvent, and in distinct contrast to high values of order parameters for other parts of the coat protein, suggesting that the DNA−protein interface is inherently dynamic on a submicrosecond time scale,[26] and that this may play a role in the observed peak splitting. Qualitative dynamics observations from $^{1}H-^{15}N$ polarization inversion spin exchange at the magic angle (PISEMA) experiments also suggest that the coat protein backbone is mostly static, with the notable exceptions of residues at the C- and N-termini and a "hinge region" which was not observed in subsequent work.[26,50,51] In summary, it seems clear from our present work and previous studies that the overall heterogeneity in the structure is low, but that in the DNA−protein interface a significant degree of static heterogeneity or dynamic disorder is present.

The above observations are relevant to an important feature of the 1PFI model of the virion: the everted conformation of the DNA.[12,21] In this model, nucleotides from the up-strand are positioned quite differently with respect to their coat protein subunits than those from the down-strand, and therefore have distinct sets of first shell contacts as well as different magnetic environments, as illustrated in Figure 6. This arises from all coat protein subunits being aligned in the same direction, while the two strands of ssDNA run in opposite directions. The resulting difference in relative nucleotide position is expected to give rise to differing chemical and magnetic environments, potentially splitting the peak for each base atom into a doublet because of its differing up- and down-strand environment. Some base atoms, due to their positions, will almost certainly be more sensitive to this effect than others, resulting in larger splittings and explaining why the relatively low resolution afforded by our DNP spectra was sufficient to see some splittings but not others.

On the basis of the Liu and Day[12] and Tsuboi et al.[21] models, the same splitting effects would be expected to hold true for the DNA sugar peaks, because each of the four bases assumes a slightly different N-glycoside torsion angle,[21] which could affect the sugar resonances differently. Therefore, in principle, it is not unreasonable to expect up to 8 resonances for each sugar carbon of the four nucleotides in each of the two strands. DFT calculations show that deoxyribose magnetic shielding anisotropy, and, by extension, chemical shifts are indeed sensitive to the glycosidic torsion angle.[76] SSNMR data on RNA nucleosides and nucleotides also supports this view.[44] Nearest-neighbor effects are highly unlikely in Pf1 DNA due to the distances involved (N9/N1 atoms of neighboring nucleotides are approximately 11.5−12.1 Å apart in the same strand and 9.4−10.4 Å apart in opposite strands); therefore, any splittings must be due to interactions with the coat protein.

Protein−DNA Interactions. The spectra presented in Figure 3 and Figures S2 and S3 contain previously undetected protein−DNA crosspeaks, namely the Y40CG-AC5 and Y40CE-AC5 protein−base crosspeaks as well as Y40CA-C1′/C4′, Y40CA-C3′, and Y40CE-C1′/C4′ protein−sugar crosspeaks at longer (200 ms) mixing times. At shorter (20 ms) mixing times, only the Y40CE-AC5 and Y40CZ-C1′ crosspeaks are observed; these are therefore presumed to be the shortest-range of the protein−DNA contacts. The presence of these contacts suggests a mechanism for aromatic stacking as suggested by observed chemical shift patterns. Further, it is consistent with the 1PFI model, which places Y40 within interaction range of the DNA, and supports the hypothesized critical role of Y40 at the protein−DNA interface.

CONCLUSIONS

The mere presence of the DNA peaks, and especially of those corresponding to the bases, indicates a well-ordered DNA structure. A number of DNA peaks are split into multiple resonances, consistent with the idea that each nucleotide type in each strand has an environment shared by all nucleotides of that type in that strand. These unique environments share common features, namely 2′-endo/*gauche* deoxyribose ring conformations and *anti* glycosidic bond orientations, corroborating conclusively results from other methods.[23] Extreme DNA chemical shift values, in some cases falling outside of BMRB chemical shift ranges, indicate an unusual DNA structure. The DNA lacks hydrogen bonding, also corroborating previous findings,[11,14,70] yet there is some sort of stacking present, consistent with predicted base−tyrosine interactions[19] and the presence of Y40-DNA (base and sugar) crosspeaks. Overall, these initial high-resolution NMR results support the Pf1 DNA model put forth by Liu and Day and subsequently refined by Tsuboi et al.[12,21]

MATERIALS AND METHODS

Uniformly ^{13}C- and ^{15}N-Labeled Pf1 Phage. The phage was prepared as previously described in Goldbourt et al.[52] The purified virus had a UV absorbance spectrum with a maximum at 270 nm, a minimum at 245 nm, and an OD_{270}/OD_{245} ratio of 1.20 ± 0.01. On the basis of an extinction coefficient of 2.1 mg^{-1} cm^{2},[24] and a molecular weight of 36 MDa, approximately 40% ± 20% of the Pf1 physical particles gave plaques in assays of infectivity on its specific host PAK.

DNA ^{13}C,^{15}N-Labeled Pf1 Phage. See Supporting Information.

DNP-NMR Sample Preparation. PEG-8000 precipitate (6 mg) of Pf1 was resuspended in a solution that consisted of 200 μL of DMSO-d_6 (Cambridge Isotope), 250 μL of D_2O (Cambridge Isotope), 50 μL of 10 mM Tris buffer (pH 8.4) [40:50:10 mixture by volume], and 20% w/v PEG-8000. The solution was made 5 mM $MgCl_2$ by the addition of 1 M stock solution, and precipitated. Pelleting was accomplished by centrifugation. The supernatant was removed and the pellet (with a volume of approximately 16 μL) transferred by centrifugation into a specially designed Bruker 3.2 mm sapphire rotor for DNP. A 220 μM stock solution of the biradical TOTAPOL[58] was added to the sample in the rotor to make it 20 μM TOTAPOL, after which the rotor was sealed.

NMR Sample Preparation. For both uniformly-^{13}C,^{15}N-labeled and DNA-^{13}C,^{15}N-labeled Pf1, 12 mg of the respectively labeled phage was precipitated from 100 mM Tris buffer (pH 8.4) using 8% w/v PEG-8000 and 5 mM $MgCl_2$. Pelleting was accomplished by 20 min centrifugation at 3700*g*. The supernatant was removed and the pellet (with a volume of approximately 40 μL) transferred by centrifugation into a standard 3.2 mm or 4 mm (Bruker or Varian) SSNMR rotor.

DNP-NMR Experiments. NMR experiments were conducted at Bruker Billerica laboratories on an AVANCE III 263 GHz solid-state DNP-NMR spectrometer ($\omega^{1}H$ = 400 MHz, 263 GHz/25 W/9.7 T gyrotron). Spectroscopy was performed by IVS, AEM, and Drs. Ansgar Siemer and Melanie Rosay. ^{13}C magnetization was prepared using a ramped cross-polarization (CP) process.[77] $^{13}C-^{13}C$ magnetization transfer during the mixing time was accomplished using the dipolar assisted rotational resonance (DARR) condition:[73] ^{13}C magnetization was stored parallel to the direction of the magnetic field while ^{1}H RF irradiation of a power matching the spinning frequency was applied.

Magnetization was then transferred to the transverse plane for detection. Mixing times of 22 and 100 ms were used to accomplish short-range (~1-bond) and long-range (~3-bond) magnetization transfers, respectively. Further experimental and processing parameters can be found in Table S1.

NMR Experiments. Solid-state NMR experiments were conducted on Bruker AVANCE II 750 MHz/17.6T and 900 MHz/21.1T spectrometers at the New York Structural Biology Center (NYSBC) as well as on Varian InfinityPlus 600 MHz/14.1T and 400 MHz/9.4T spectrometers; additional information is available in Table S1. ^{13}C magnetization was prepared using a ramped cross-polarization (CP) process.[77] $^{13}C-^{13}C$ magnetization transfer during the mixing time was accomplished using the dipolar assisted rotational resonance (DARR) condition:[73] ^{13}C magnetization was stored parallel to the direction of the magnetic field while ^{1}H RF irradiation of a power matching the spinning frequency was applied. Magnetization was then transferred to the transverse plane for detection. Mixing times of 20−50 ms were used to accomplish short 1−2 bond magnetization transfers and 200 ms for longer-range transfers.

Data Analysis. All spectra were processed using a combination of the Topspin 2.1 software (Bruker Biospin, Fremont, CA) and NMRPipe,[78] and then assigned using Sparky.[79] ^{13}C chemical shifts were referenced externally to the adamantane CH_2 peak at 40.48 ppm (relative to DSS).[80] ^{15}N chemical shifts were referenced externally to the NH_4Cl peak at 39.27 ppm.

■ ASSOCIATED CONTENT

Supporting Information. Acquisition and processing parameters for all spectra; full DNP-enhanced DARR (2D) spectrum with 22 ms mixing time of U-^{13}C,^{15}N Pf1; full 400 MHz U-^{13}C,^{15}N Pf1 DARR (2D) spectrum with 200 ms mixing time at −35 °C; 900 MHz U-^{13}C,^{15}N Pf1 DARR (2D) spectrum, with 20 ms mixing time at −60 °C − DNA regions and assignments shown; 750 MHz U-^{13}C,^{15}N Pf1 DARR (2D) spectrum with 50 ms mixing time at −30 °C − DNA regions and assignments shown; full DNA-^{13}C,^{15}N-labeled Pf1 DARR (2D) spectrum with 50 ms mixing time at −30 °C; overlay of DNP and non-DNP ^{13}C one-dimensional cross-polarization spectra illustrating DNP enhancement; comparison of CP-DARR and 1pulse-DARR spectra showing differential signal intensity; listing of data sources for database of B-DNA chemical shifts used for comparative purposes; preparation of DNA-^{13}C,^{15}N-labeled Pf1; complete ref 9; complete ref 56. This material is available free of charge via the Internet at http://pubs.acs.org.

■ AUTHOR INFORMATION

Corresponding Author
aem5@columbia.edu

■ ACKNOWLEDGMENT

This work was supported by a grant from the National Science Foundation: MCB 0316248. The authors wish to thank Drs. Ansgar Siemer and Melanie Rosay for their contributions to this project, namely in the collection of DNP-SSNMR data. The authors would also like to thank Dr. Masamichi Tsuboi for graciously providing unpublished coordinates. This work was made possible by material support from the Bruker Biospin Corporation. A.G. is supported by the Israel Science Foundation and a Marie-Curie reintegration grant (EU-FP7-IRG).

■ REFERENCES

(1) Takeya, K.; Amako, K. *Virology* **1966**, *28* (1), 163–7.
(2) Davis, B. M.; Waldor, M. K. Virulence-linked bacteriophages of pathogenic vibrios. In *Phages: Their Role in Bacterial Pathogenesis and Biotechnology*; Waldor, M. K., Freidman, D. I., Adhya, S. L., Eds.; ASM Press: Washington, DC, 2005; pp 187−205.
(3) Gonzalez, M. D.; Lichtensteiger, C. A.; Caughlan, R.; Vimr, E. R. *J. Bacteriol.* **2002**, *184* (21), 6050–5.
(4) Day, L. A. Inoviruses. In *Encyclopedia of Virology*; Mahy, B. W. J., van-Regenmortel, M. H. V., Eds.; Elsevier: Oxford, 2008; Vol. 1, pp 117−124.
(5) Kuo, T. T.; Lin, Y. H.; Huang, C. M.; Chang, S. F.; Dai, H.; Feng, T. Y. *Virology* **1987**, *156* (2), 305–12.
(6) Waldor, M. K.; Mekalanos, J. J. *Science* **1996**, *272* (5270), 1910–4.
(7) Rice, S. A.; Tan, C. H.; Mikkelsen, P. J.; Kung, V.; Woo, J.; Tay, M.; Hauser, A.; McDougald, D.; Webb, J. S.; Kjelleberg, S. *ISME J.* **2009**, *3* (3), 271–82.
(8) Webb, J. S.; Lau, M.; Kjelleberg, S. *J. Bacteriol.* **2004**, *186* (23), 8066–73.
(9) Winstanley, C.; et al. *Genome Res.* **2009**, *19* (1), 12–23.
(10) Hill, D. F.; Short, N. J.; Perham, R. N.; Petersen, G. B. *J. Mol. Biol.* **1991**, *218* (2), 349–64.
(11) Day, L. A.; Marzec, C. J.; Reisberg, S. A.; Casadevall, A. *Annu. Rev. Biophys. Biophys. Chem.* **1988**, *17*, 509–39.
(12) Liu, D. J.; Day, L. A. *Science* **1994**, *265* (5172), 671–674.
(13) Marvin, D. A. *Curr. Opin. Struct. Biol.* **1998**, *8* (2), 150–158.
(14) Casadevall, A.; Day, L. A. *Nucleic Acids Res.* **1982**, *10* (7), 2467–2481.
(15) Kostrikis, L. G.; Liu, D. J.; Day, L. A. *Biochemistry* **1994**, *33* (7), 1694–703.
(16) Tomar, S.; Green, M. M.; Day, L. A. *J. Am. Chem. Soc.* **2007**, *129* (11), 3367–3375.
(17) Wiseman, R. L.; Day, L. A. *J. Mol. Biol.* **1977**, *116* (3), 607–611.
(18) Bryan, R. K.; Bansal, M.; Folkhard, W.; Nave, C.; Marvin, D. A. *Proc. Natl. Acad. Sci. U.S.A.* **1983**, *80* (15), 4728–4731.
(19) Day, L. A.; Wiseman, R. L.; Marzec, C. J. *Nucleic Acids Res.* **1979**, *7* (6), 1393–403.
(20) Marzec, C. J.; Day, L. A. *Biophys. J.* **1994**, *67* (6), 2205–2222.
(21) Tsuboi, M.; Tsunoda, M.; Overman, S. A.; Benevides, J. M.; Thomas, G. J. *Biochemistry* **2010**, *49* (8), 1737–43.
(22) Tsuboi, M.; Benevides, J. M.; Thomas, G. J. *Proc. Jpn. Acad., Ser. B* **2009**, *85* (3), 83–97.
(23) Tsuboi, M.; Kubo, Y.; Ikeda, T.; Overman, S. A.; Osman, O.; Thomas, G. J., Jr. *Biochemistry* **2003**, *42* (4), 940–50.
(24) Allemand, J. F.; Bensimon, D.; Lavery, R.; Croquette, V. *Proc. Natl. Acad. Sci. U.S.A.* **1998**, *95* (24), 14152–14157.
(25) Smith, S. B.; Cui, Y. J.; Bustamante, C. *Science* **1996**, *271* (5250), 795–799.
(26) Lorieau, J. L.; Day, L. A.; McDermott, A. E. *Proc. Natl. Acad. Sci. U.S.A.* **2008**, *105* (30), 10366–71.
(27) Tycko, R. *Prog. Nucl. Magn. Reson. Spectrosc.* **2003**, *42* (1−2), 53–68.
(28) Straus, S. K. *Philos. Trans. R. Soc., B* **2004**, *359* (1446), 997–1008.
(29) McDermott, A. E. *Curr. Opin. Struct. Biol.* **2004**, *14* (5), 554–561.
(30) Baldus, M. *Prog. Nucl. Magn. Reson. Spectrosc.* **2002**, *41* (1−2), 1–47.
(31) Igumenova, T. I.; Wand, A. J.; McDermott, A. E. *J. Am. Chem. Soc.* **2004**, *126* (16), 5323–5331.
(32) Igumenova, T. I.; McDermott, A. E.; Zilm, K. W.; Martin, R. W.; Paulson, E. K.; Wand, A. J. *J. Am. Chem. Soc.* **2004**, *126* (21), 6720–6727.
(33) Franks, W. T.; Zhou, D. H.; Wylie, B. J.; Money, B. G.; Graesser, D. T.; Frericks, H. L.; Sahota, G.; Rienstra, C. M. *J. Am. Chem. Soc.* **2005**, *127* (35), 12291–12305.
(34) Siemer, A. B.; Ritter, C.; Steinmetz, M. O.; Ernst, M.; Riek, R.; Meier, B. H. *J. Biomol. NMR* **2006**, *34* (2), 75–87.

(35) van Gammeren, A. J.; Hulsbergen, F. B.; Hollander, J. G.; de Groot, H. J. M. *J. Biomol. NMR* **2005**, *31* (4), 279–293.
(36) Lange, A.; Becker, S.; Seidel, K.; Giller, K.; Pongs, O.; Baldus, M. *Angew. Chem., Int. Ed.* **2005**, *44* (14), 2089–2092.
(37) Bockmann, A.; Lange, A.; Galinier, A.; Luca, S.; Giraud, N.; Juy, M.; Heise, H.; Montserret, R.; Penin, F.; Baldus, M. *J. Biomol. NMR* **2003**, *27* (4), 323–339.
(38) Marulanda, D.; Tasayco, M. L.; Cataldi, M.; Arriaran, V.; Polenova, T. *J. Phys. Chem. B* **2005**, *109* (38), 18135–18145.
(39) McDermott, A.; Polenova, T.; Bockmann, A.; Zilm, K. W.; Paulsen, E. K.; Martin, R. W.; Montelione, G. T. *J. Biomol. NMR* **2000**, *16* (3), 209–219.
(40) Wylie, B. J.; Franks, T.; Graesser, D. T.; Rienstra, C. M. *J. Am. Chem. Soc.* **2005**, *127* (34), 11946–11947.
(41) Ladizhansky, V.; Jaroniec, C. P.; Diehl, A.; Oschkinat, H.; Griffin, R. G. *J. Am. Chem. Soc.* **2003**, *125* (22), 6827–6833.
(42) Castellani, F.; van Rossum, B.; Diehl, A.; Schubert, M.; Rehbein, K.; Oschkinat, H. *Nature* **2002**, *420* (6911), 98–102.
(43) Zech, S. G.; Wand, A. J.; McDermott, A. E. *J. Am. Chem. Soc.* **2005**, *127* (24), 8618–8626.
(44) Ebrahimi, M.; Rossi, P.; Rogers, C.; Harbison, G. S. *J. Magn. Reson.* **2001**, *150* (1), 1–9.
(45) Olsen, G. L.; Louie, E. A.; Drobny, G. P.; Sigurdsson, S. T. *Nucleic Acids Res.* **2003**, *31* (17), 5084–5089.
(46) Riedel, K.; Herbst, C.; Hafner, S.; Leppert, J.; Ohlenschlaeger, O.; Swanson, M. S.; Gorlach, M.; Ramachandran, R. *Angew. Chem., Int. Ed.* **2006**, *45* (34), 5620–5623.
(47) Juang, C. L.; Tang, P.; Harbison, G. S. *Methods Enzymol.* **1995**, *261*, 256–270.
(48) Oyler, N. A. SSNMR methods for determining structure in nucleosides and peptides. Ph.D. Thesis, University of Washington, 2000.
(49) Cherepanov, A. V.; Glaubitz, C.; Schwalbe, H. *Angew. Chem., Int. Ed.* **2010**, *49* (28), 4747–4750.
(50) Thiriot, D. S.; Nevzorov, A. A.; Zagyanskiy, L.; Wu, C. H.; Opella, S. J. *J. Mol. Biol.* **2004**, *341* (3), 869–79.
(51) Thiriot, D. S.; Nevzorov, A. A.; Opella, S. J. *Protein Sci.* **2005**, *14* (4), 1064–1070.
(52) Goldbourt, A.; Gross, B. J.; Day, L. A.; McDermott, A. E. *J. Am. Chem. Soc.* **2007**, *129* (8), 2338–44.
(53) Cross, T. A.; Tsang, P.; Opella, S. J. *Biochemistry* **1983**, *22* (4), 721–6.
(54) Magusin, P. C.; Hemminga, M. A. *Biophys. J.* **1993**, *64* (6), 1861–8.
(55) Rosay, M.; Zeri, A. C.; Astrof, N. S.; Opella, S. J.; Herzfeld, J.; Griffin, R. G. *J. Am. Chem. Soc.* **2001**, *123* (5), 1010–1.
(56) Ulrich, E. L.; et al. *Nucleic Acids Res.* **2008**, *36* (Database issue), D402-8.
(57) Germann, M. W. Nucleic Acids NMR Spectroscopy, http://tesla.ccrc.uga.edu/courses/BioNMR2006/lectures/march20.pdf, (accessed Aug. 21, 2010). Course: Nuclear Magnetic Resonance Spectroscopy of Biomolecules, University of Georgia, 2006.
(58) Song, C.; Hu, K. N.; Joo, C. G.; Swager, T. M.; Griffin, R. G. *J. Am. Chem. Soc.* **2006**, *128* (35), 11385–90.
(59) Lankhorst, P. P.; Erkelens, C.; Haasnoot, C. A.; Altona, C. *Nucleic Acids Res.* **1983**, *11* (20), 7215–30.
(60) Santos, R. A.; Tang, P.; Harbison, G. S. *Biochemistry* **1989**, *28* (24), 9372–9378.
(61) Xu, X.-P.; Chiu, W.-L. A. K.; Au-Yeung, S. C. F. *J. Am. Chem. Soc.* **1998**, *120*, 4230–4231.
(62) Greene, K. L.; Wang, Y.; Live, D. *J. Biomol. NMR* **1995**, *5* (4), 333–8.
(63) Ghose, R.; Marino, J. P.; Wiberg, K. B.; Prestegard, J. H. *J. Am. Chem. Soc.* **1994**, *116* (19), 8827–8828.
(64) Lam, S. L.; Chi, L. M. *Prog. Nucl. Magn. Reson. Spectrosc.* **2010**, *56* (3), 289–310.
(65) Borer, P. N.; LaPlante, S. R.; Zanatta, N.; Levy, G. C. *Nucleic Acids Res.* **1988**, *16* (5), 2323–32.
(66) LaPlante, S. R.; Boudreau, E. A.; Zanatta, N.; Levy, G. C.; Borer, P. N.; Ashcroft, J.; Cowburn, D. *Biochemistry* **1988**, *27* (20), 7902–9.
(67) Fares, C.; Amata, I.; Carlomagno, T. *J. Am. Chem. Soc.* **2007**, *129* (51), 15814–23.
(68) Malinakova, K.; Novosadova, L.; Lahtinen, M.; Kolehmainen, E.; Brus, J.; Marek, R. *J. Phys. Chem. A* **2010**, *114* (4), 1985–95.
(69) Zhang, X. H.; Gaffney, B. L.; Jones, R. A. *J. Am. Chem. Soc.* **1998**, *120* (26), 6625–6626.
(70) Day, L. A.; Casadevall, A.; Prescott, B.; Thomas, G. J. *Biochemistry* **1988**, *27* (2), 706–711.
(71) Pletneva, E. V.; Laederach, A. T.; Fulton, D. B.; Kostic, N. M. *J. Am. Chem. Soc.* **2001**, *123* (26), 6232–6245.
(72) Bajaj, V. S.; Farrar, C. T.; Hornstein, M. K.; Mastovsky, I.; Vieregg, J.; Bryant, J.; Elena, B.; Kreischer, K. E.; Temkin, R. J.; Griffin, R. G. *J. Magn. Reson.* **2003**, *160* (2), 85–90.
(73) Takegoshi, K.; Nakamura, S.; Terao, T. *Chem. Phys. Lett.* **2001**, No. 344, 631–637.
(74) Hu, K. N.; Yau, W. M.; Tycko, R. *J. Am. Chem. Soc.* **2010**, *132* (1), 24–5.
(75) Gross, B. Three dimensional structure determination for single crystal and uniaxially aligned amino acids by magic angle spinning solid-state NMR. Ph.D. Thesis, Columbia University, New York, NY, 2004.
(76) Brumovska, E.; Sychrovsky, V.; Vokacova, Z.; Sponer, J.; Schneider, B.; Trantirek, L. *J. Biomol. NMR* **2008**, *42* (3), 209–23.
(77) Kawashima, H.; Yamada, O. *Fuel Process. Technol.* **1999**, *61* (3), 279–287.
(78) Delaglio, F.; Grzesiek, S.; Vuister, G. W.; Zhu, G.; Pfeifer, J.; Bax, A. *J. Biomol. NMR* **1995**, *6* (3), 277–293.
(79) Goddard, T. D.; Kneller, D. G. *SPARKY 3.110*; University of California: San Francisco, CA, 2004.
(80) Morcombe, C. R.; Zilm, K. W. *J. Magn. Reson.* **2003**, *162* (2), 479–486.